J. Fluid Mech. (1972), *vol.* 53, *part* 1, *pp.* 45–60
Printed in Great Britain

A note on von Kármán's constant in low Reynolds number turbulent flows

By G. DAVID HUFFMAN† AND PETER BRADSHAW
Department of Aeronautics, Imperial College, London

(Received 15 June 1971)

An analysis of existing data on low Reynolds number flows strongly suggests that the conclusion of Simpson (1970) concerning the variation of von Kármán's constant k with Reynolds number is not correct. This implies that Coles' (1962) assumption of the validity of the logarithmic velocity profile at low Reynolds numbers *is* correct and, moreover, that the inference drawn by Coles and later authors regarding the presence of viscous effects in the outer layer is valid. The analysis shows that these viscous effects are not present in duct flows, so that they are presumably associated with the presence of a turbulent–irrotational interface; it is argued that the 'viscous superlayer' can affect a large part of the outer layer at low Reynolds numbers. The data analysis incidentally shows that the viscous *sublayer* is more strongly affected by shear-stress gradients or transverse wall curvature than is the rest of the inner layer.

1. Introduction

Coles (see Coles 1962; Coles & Hirst 1968) analysed the bulk of available measurements of turbulent boundary layers with low Reynolds number and in zero pressure gradients. He determined the surface shear stress from the velocity profile by assuming that the velocity in the inner layer ($y/\delta \lesssim 0{\cdot}2$) but outside the viscous sublayer ($u_\tau y/\nu \gtrsim 40$) followed the usual logarithmic form

$$\frac{u}{u_\tau} = \frac{1}{k}\log\frac{u_\tau y}{\nu} + C, \tag{1}$$

where $k = 0{\cdot}41$ and $C = 5{\cdot}0$. Coles found that the velocity defect formula

$$(u_e - u)/u_\tau = f_1(y/\delta) \tag{2}$$

in the outer part of the boundary layer ($y/\delta \lesssim 0{\cdot}2$) was a function of the Reynolds number for momentum-thickness Reynolds numbers Re_θ of less than about 5000. In particular, Coles' 'wake' profile parameter Π, or $\frac{1}{2}k\Delta u/u_\tau$, where Δu is defined in figure 1, fell from about 0·6 at high Reynolds numbers to zero for Reynolds numbers of approximately 500. Note that Coles & Hirst's 1968 analysis of the data of Wieghardt, which appears to be representative of the low Reynolds number data in general, gives slightly different results from the 1962 analysis and is presumably to be regarded as superseding the latter. Coles briefly discussed the

† Present address: Detroit Diesel Allison Division, General Motors Corporation, Indianapolis.

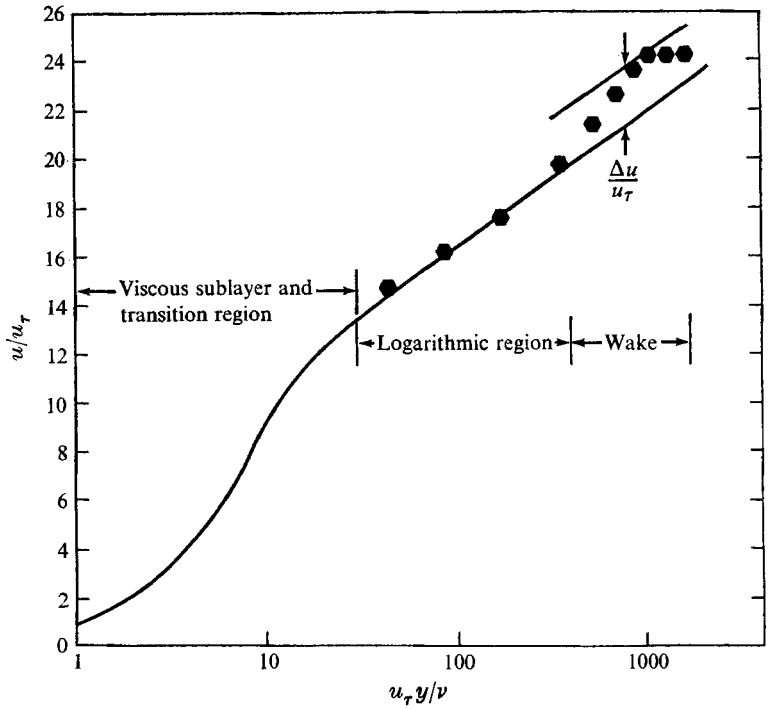

FIGURE 1. The 'law of the wall' and 'law of the wake' for a typical turbulent boundary layer.

validity of the logarithmic law (1) and demonstrated that the surface shear stress deduced from it was within about 10% of that deduced from the momentum integral equation, at least in the case of the more reliable experiments.

The modern derivation of the 'mixing-length' formula, from which (1) follows by integration when $\tau/\rho = u_\tau^2 \equiv \tau_w/\rho$, uses the assumption that the turbulent structure of the flow near the surface is unaffected by the flow further from the surface (Townsend 1961). This formula seems to be valid over a wide range of outer-layer conditions, and the Kármán–Schoenherr skin friction formula derived from (1) and (2) is valid up to very high Reynolds numbers. The outer layer and outer boundary conditions affect the inner layer primarily via the shear-stress gradient $\partial\tau/\partial y$ in the inner layer, which is non-zero when the flow and/or pressure are functions of x. In a constant-pressure boundary layer at $Re_\theta = 1000$, the effect of $\partial\tau/\partial y$ is to reduce the velocity gradient at $y/\delta = 0{\cdot}1$ by about 3 per cent from that in a true constant-stress layer; that is, the apparent value of k in (1) increases by 3 per cent. Townsend (1961) discusses certain anomalies in the turbulence structure (the 'inactive motion') but concludes that these effects are more important at high Reynolds numbers than at low ones and should not in any event alter the 'mixing length'. The validity in the inner layer of the mixing-layer formula and the resulting logarithmic law is generally accepted while the source of the supposed outer-layer effects at low Reynolds number is primarily speculative.

Simpson (1970) suggested that much larger changes in the logarithmic law

occurred at low Reynolds numbers. He showed that his own velocity profiles, and those of Wieghardt, for $1000 < Re_\theta < 6000$ collapse together, except in the viscous sublayer, when plotted as u/u_e versus y/δ. Since $u_\tau/u_e \equiv (\frac{1}{2}C_f)^{\frac{1}{2}} \propto Re_\theta^{-\frac{1}{8}}$ approximately, it follows that k varies as $Re_\theta^{-\frac{1}{8}}$, decreasing to 0·33 at $Re_\theta = 1000$; C also varies. There is therefore a direct contradiction between the analyses of Wieghardt's data by Coles (constant k) and by Simpson (variable k). Recently Cebeci & Mosinskis (1970), following Simpson, used values of k and C varying with Re_θ as part of the input to a method of calculating turbulent boundary layers and showed improved agreement with experimental data. On the other hand Herring & Mellor (1968), using a very similar calculation method, obtained improved agreement by letting the eddy viscosity in the outer layer depend on Reynolds number, leaving k and C unaltered. Again we have a direct contradiction: it seems that the boundary-layer data currently available are not accurate enough to check the validity of the logarithmic law at low Reynolds numbers. Nevertheless, the question is of some importance, if only because of the implications for the inner-layer analysis in other situations.

In § 2 of this paper we present an analysis of data for flows in which Reynolds number effects on the inner layer are likely to be *stronger* than in a boundary layer, and thus easier to detect. The procedure adopted is to adjust k and the 'damping constant' A^+, which determines C, so as to optimize the agreement between the actual velocity profiles in the inner layer and those calculated from the mixing-length formula. The results show that C or its equivalent is Reynolds number dependent and that k appears to be a constant to good accuracy. It appears that even the variation of C is likely to be small in boundary layers unless the influence of the outer layer is extremely large.

Accepting that this is the best vindication of the logarithmic law that current data are likely to provide, it is shown in § 3 that velocity defect profiles in ducts do follow equation (2) at low Reynolds numbers even though the boundary-layer defect profiles do not. This paradox is at once resolved if it is supposed that the Reynolds number (viscous) effects in the boundary layer are associated with the presence of an irrotational–turbulent interface and in particular with the viscous superlayer (Corrsin & Kistler 1955). A conservative estimate of the superlayer thickness suggests that it may occupy a large fraction of the outer region of a boundary layer at low Reynolds numbers, whereas it is of course absent in ducts. Another possibility, sensitivity to $d\delta/dx$, seems less plausible.

In § 4, the *status quo* is restored by presenting an incidental result from the present analysis, showing that transverse curvature affects the viscous sublayer appreciably even when the ratio of sublayer thickness to radius of curvature is as small as 0·1. The flow in the inner layer but outside the sublayer is apparently unaffected by transverse curvature. Therefore, we have acquitted the inner layer of violating the logarithmic law at low Reynolds numbers only to find evidence of its misbehaviour in other circumstances, admittedly less important ones.

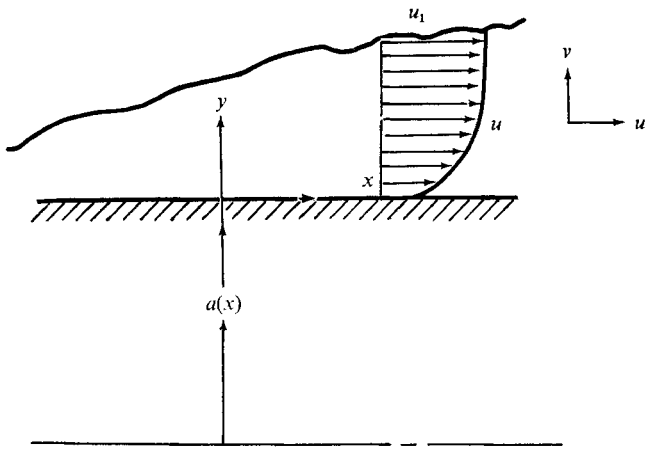

FIGURE 2. Flow field geometry.

2. Analysis of velocity profiles in low Reynolds number flows

2.1. *Calculation of the shear-stress profile*

A major difficulty in analysing low Reynolds number flows other than duct flows is that adequate measurements of the shear stress τ are seldom available, so that τ must be calculated from measured velocity profiles by using the equation of motion. Values of u_τ and du_τ/dx are also needed. In duct flows (on which the conclusions of this paper mainly depend) u_τ is known from the pressure drop and du_τ/dx is zero, but in the other flows we have analysed u_τ has been obtained directly or indirectly from conditions in the viscous sublayer. Our velocity profiles calculated using the measured u_τ agree sufficiently well with the measured profiles in the sublayer to justify the u_τ values *a posteriori*.

The assumption that the turbulent flow near a smooth solid surface (y/δ or $y/a < 0{\cdot}2$) depends only on u_τ, y, ρ and ν leads via similarity arguments and dimensional analysis to

$$u = u_\tau f_2(\zeta), \tag{3}$$

where

$$\zeta = (u_\tau y/\nu)\,(1+y/2a)^i \tag{4}$$

and f_2 is a universal function of ζ, a is the radius of the bounding surface (see figure 2) and i takes on the values of 0 and 1 for two-dimensional and axisymmetric flow fields respectively. The axisymmetric formulation is presented by Willmarth & Yang (1970) as a recapitulation of prior unpublished work; like (3), it is not uncontroversial, but should suffice for calculating the shear-stress profile from given velocity profiles.

Equations (3) and (4) in conjunction with the momentum and continuity relations

$$\rho u\frac{\partial u}{\partial x}+\rho v\frac{\partial u}{\partial y} = -\frac{dp}{dx}+\frac{1}{(a+y)^i}\frac{\partial}{\partial y}[(a+y)^i\tau] \tag{5}$$

and

$$\frac{\partial}{\partial x}[(a+y)^i\rho u]+\frac{\partial}{\partial y}[(a+y)^i\rho v] = 0 \tag{6}$$

yield an equation for the total (viscous plus turbulent) shear stress as a function of distance from the surface and a number of parameters.

We have

$$(1+y^+/a^+)^i\tau^+ = 1+\pi^+y^+(1+y^+/2a^+)^i+v_w^+(u^+-u_w^+) + \frac{d(\log u_\tau)}{dx^+}\int_0^{y^+} u^{+2}(1+y^+/a^+)^i\,dy^+, \tag{7}$$

where $y^+ = yu_\tau/\nu$, $a^+ = au_\tau/\nu$, $\tau^+ = \tau/\tau_w$, $\pi^+ = (\nu/\rho u_\tau^3)\,dp/dx$

$$v^+ = v/u_\tau, \quad u^+ = u/u_\tau, \quad dx^+ = u_\tau\,dx/\nu,$$

and the subscript w denotes conditions at the wall. The gradient $\partial\tau^+/\partial y^+$ can be obtained from (5) or (7). Retaining terms of degree $(i-1)$ for clarity, we get

$$\left(1+\frac{y^+}{a^+}\right)^i\frac{\partial\tau^+}{\partial y^+} = \pi^+\left(1+\frac{y^+}{2a^+}\right)^i+\frac{i\pi^+y^+}{2a^+}\left(1+\frac{y^+}{2a^+}\right)^{i-1} + v_w^+\frac{\partial u^+}{\partial y^+}+\frac{d(\log u_\tau)}{dx^+}u^{+2}\left(1+\frac{y^+}{a^+}\right)^i-\frac{i\tau^+}{a^+}\left(1+\frac{y^+}{a^+}\right)^{i-1}. \tag{8}$$

Note that $\partial\tau^+/\partial y^+$ at given y^+ is a function of π^+, a^+, v_w^+ and $d(\log u_\tau)/dx^+$.

2.2. *Optimization of the mixing-length distribution*

The total shear stress can be related to the velocity gradient via

$$\tau^+ = \frac{\partial u^+}{\partial y^+}+\left(l^+\frac{\partial u^+}{\partial y^+}\right)^2, \tag{9}$$

which can be taken as a definition of the 'mixing length' l, where $l^+ = u_\tau l/\nu$. The common assumption that l is proportional to y can be justified by local-equilibrium arguments within the inner layer but outside the viscous sublayer. Equation (9) has also been used in the viscous sublayer (which is not a local-equilibrium region because significant turbulent energy transport normal to the surface occurs) but its status is simply that of a means of correlating data. Van Driest (1956) showed that, for the simple case $\tau^+ =$ constant $= \tau_w^+$, experimental velocity profiles were well fitted throughout the inner layer by the semi-empirical form

$$l^+ = ky^+\{1-\exp[-\tau^{+\frac{1}{2}}y^+/A^+]\}, \tag{10}$$

which tends to $l^+ = ky^+$ for large y^+, and this form was used for cases where $\tau^+ \neq \tau_w^+$ by Patankar & Spalding (1967) and Cebeci & Smith (1968). Closely similar expressions were used by Herring & Mellor (1968) and McDonald (1969). If $\tau^+ = \tau_w^+$, equation (9), with the substitution (10), integrates to give (1) for $y^+ > 10$ (say), and the constant C depends uniquely on, and increases with, A^+; $A^+ = 26$ gives $C = 5$. If $\tau^+ \neq \tau_w^+$ (i.e. $\partial\tau^+/\partial y^+ \neq 0$), (1) becomes more complicated, C or its equivalent depends on $\partial\tau^+/\partial y^+$ and there is no good reason to suppose that A^+ remains equal to 26. However (as will be shown below) (9) with (10) still gives a good fit to experimental velocity profiles in the inner layer and the 'profile parameters' A^+ and k are still useful measures of profile behaviour, A^+ being more convenient for discussion purposes than C because of the different forms of (1) in different cases.

In the present analysis, (9) rearranged in the form

$$\frac{\partial u^+}{\partial y^+} = \frac{(1+4l^{+2}\tau^+)^{\frac{1}{2}}-1}{2l^{+2}}, \tag{11}$$

with substitutions from (7) and (10), has been integrated and fitted to a number of experimental velocity profiles in different turbulent wall flows at low Reynolds numbers. k and A^+ have been chosen to give the best fit in the region between the surface and the expected outer limit of validity of (10), generally about 20 % of the flow width; that is, the points at large y^+ in figures 3–8 have been ignored. The optimum values were found numerically by means of a logical search algorithm described by Huffman (1971).

Simpson (1970) suggested that in the low Reynolds number boundary layer C (or A^+) varied as k varied, in such a way as to give approximate similarity in y^+, u^+ co-ordinates in the logarithmic region, as well as (even more accurate) similarity in y/δ, u/u_e co-ordinates. We regard his suggestion as far-fetched; the success of the local-similarity analysis for the inner layer in cases where the outer layer is highly turbulent makes it unlikely that the inner layer will depend on the outer layer in the less demanding case of a constant-pressure boundary layer. Even if one concedes that local similarity will eventually break down at Reynolds numbers so low that the flow is not completely turbulent, the chances of the effects on k and C extending to R_θ as high as 6000 *and* compensating each other so that the profile remains almost unchanged are remote indeed. It was remarked some time ago by Black & Sarnecki (1958) that different experimental determinations of k and C for a given flow can be quite widely (and randomly) scattered and yet agree closely on the velocity profile within the rather small logarithmic region. We could find no trace of a consistent trend of k with Reynolds number in the flows we analysed, even though some of them exhibited strong Reynolds number effects on A^+; the optimum value of k seemed to be close to 0·41 and so we adopted this *constant value of k* for the analysis presented here. This does *not* prejudge the question of changes in the logarithmic-law constants. If the value of k were varied but k assumed constant in the profile fitting process one would expect the optimum A^+ to vary to compensate. If this optimum A^+ were found to be *constant* even in the presence of rather stronger Reynolds number effects than those found in low Reynolds number boundary layers then the traditional assumptions of constant A^+ (or C) *and* constant k would be confirmed with fairly high probability. This was found to be the case in the profile fits to be described below; A^+ does, however, vary in flows subject to much stronger Reynolds number effects than the boundary layer.

As long as the flow is fully turbulent, the leading parameter representing external effects on the inner layer and leading to departures from the form (1) is expected to be $\partial\tau^+/\partial y^+$ or, in plain symbols, $(\nu/\rho u_\tau^3)\,\partial\tau/\partial y$; either this parameter or $(\nu/\rho u_\tau^3)\,\partial p/dx$ or $(\nu/U_e^2)\,dU_e/dx \equiv (\frac{1}{2}c_f)^{\frac{3}{2}}(\nu/\rho u_\tau^3)\,dp/dx$ are commonly used in discussions of reverse transition, which is the ultimate in 'low Reynolds number' effects. In practice $\partial\tau/\partial y$ is not quite independent of y in the inner layer of developing flows, so we have plotted the results of our data fits in figures 6–8 in the form

$$u^+ = f_3(y^+, \langle\partial\tau^+/\partial y^+\rangle), \tag{12}$$

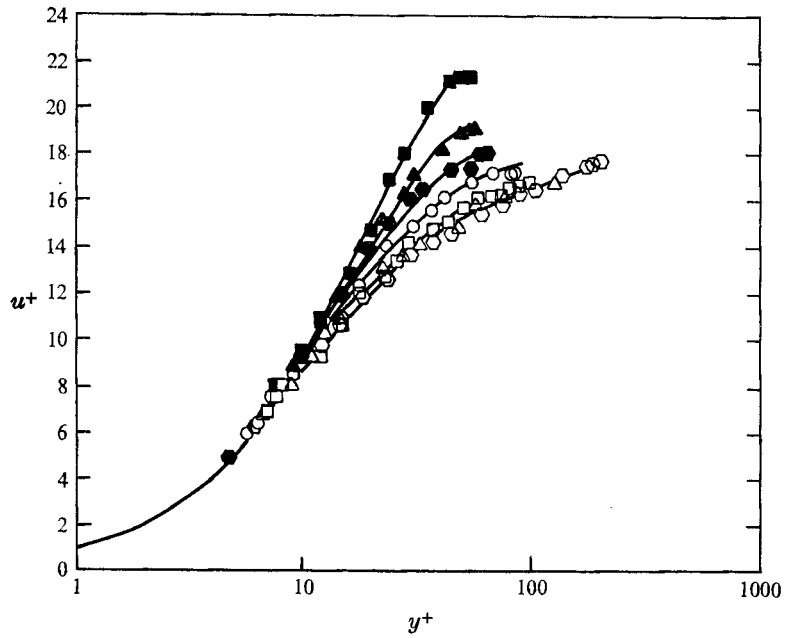

FIGURE 3. Fully developed channel flow (Patel & Head 1969). ○, $\langle \partial\tau^+/\partial y^+ \rangle = -0{\cdot}0049$, $A^+ = 30$; △, $\langle \partial\tau^+/\partial y^+ \rangle = -0{\cdot}008$, $A^+ = 32$; □, $\langle \partial\tau^+/\partial y^+ \rangle = -0{\cdot}010$, $A^+ = 36$; ○, $\langle \partial\tau^+/\partial y^+ \rangle = -0{\cdot}013$, $A^+ = 45$; ●, $\langle \partial\tau^+/\partial y^+ \rangle = -0{\cdot}015$, $A^+ = 61$; ▲, $\langle \partial\tau^+/\partial y^+ \rangle = -0{\cdot}017$, $A^+ = 80$; ■, $\langle \partial\tau^+/\partial y^+ \rangle = -0{\cdot}019$, $A^+ = 140$; —, computed velocities.

where the second parameter is the average shear-stress gradient over the range of integration of (11), defined by

$$\left\langle \frac{\partial\tau^+}{\partial y^+} \right\rangle = \frac{\int_0^{y^+_{\max}} \left(1+\frac{y^+}{a^+}\right)^i \left(\frac{\partial\tau^+}{\partial y^+}\right) dy^+}{\int_0^{y^+_{\max}} \left(1+\frac{y^+}{a^+}\right)^i dy^+}. \tag{13}$$

The effect of external conditions on u^+ is transmitted either by $\langle \partial\tau^+/\partial y^+ \rangle$ or by alterations in the u^+ boundary condition. Again $\langle \partial\tau^+/\partial y^+ \rangle$ depends on π^+, a^+, v_w^+ and/or $d \log u_\tau/dx^+$.

The data of Patel & Head (1969) dealing with low Reynolds number flows in circular pipes and two-dimensional ducts are shown in figures 3 and 4. In this case, the dimensionless shear-stress gradient is constant and equals $-1/a^+$, where a is the pipe radius or the duct half-width. The duct Reynolds number based on the mean velocity, i.e. $2a\bar{u}/\nu$, can be related to $\langle \partial\tau^+/\partial y^+ \rangle$ and is approximately $-30/\langle \partial\tau^+/\partial y^+ \rangle$ at the Reynolds numbers of interest. It can be seen that in fully developed duct flows equation (12) is *independent* of any inner-layer considerations since it simply states that the dimensionless velocity is a function of Reynolds number and position. In other flows, the inner-layer arguments are sufficiently well established for us to accept $\partial\tau^+/\partial y^+$ as representing the major effect on external conditions on the inner layer even when $\partial\tau^+/\partial y^+$ is not uniquely determined by the Reynolds number. This appears to be the case in practice and this behaviour is illustrated in figures 5–8.

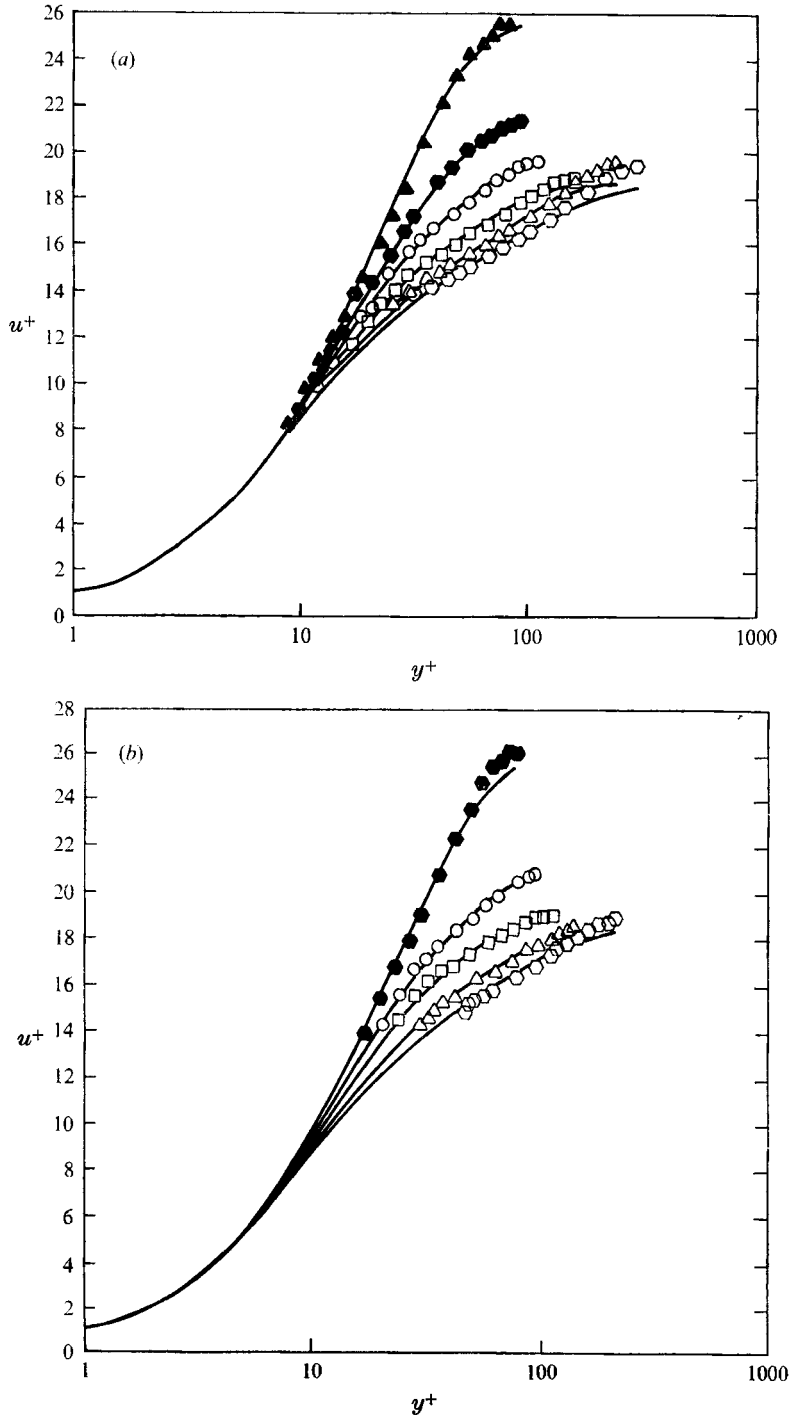

FIGURE 4. Fully developed pipe flow (Patel & Head 1969). (*a*) ⬡, $\langle \partial\tau^+/\partial y^+ \rangle = -0{\cdot}0034$, $A^+ = 31$; △, $\langle \partial\tau^+/\partial y^+ \rangle = -0{\cdot}0042$, $A^+ = 34$; □, $\langle \partial\tau^+/\partial y^+ \rangle = -0{\cdot}0065$, $A^+ = 40$; ○, $\langle \partial\tau^+/\partial y^+ \rangle = -0{\cdot}0092$, $A^+ = 52$; ⬢, $\langle \partial\tau^+/\partial y^+ \rangle = -0{\cdot}011$, $A^+ = 73$; ▲, $\langle \partial\tau^+/\partial y^+ \rangle = -0{\cdot}012$, $A^+ = 130$; —, computed velocities. (*b*) ⬡, $\langle \partial\tau^+/\partial y^+ \rangle = -0{\cdot}00465$, $A^+ = 33$; △, $\langle \partial\tau^+/\partial y^+ \rangle = -0{\cdot}0070$, $A^+ = 39$; □, $\langle \partial\tau^+/\partial y^+ \rangle = -0{\cdot}0089$, $A^+ = 50$; ○, $\langle \partial\tau^+/\partial y^+ \rangle = -0{\cdot}010$, $A^+ = 67$; ⬢, $\langle \partial\tau^+/\partial y^+ \rangle = -0{\cdot}012$, $A^+ = 130$; —, computed velocities.

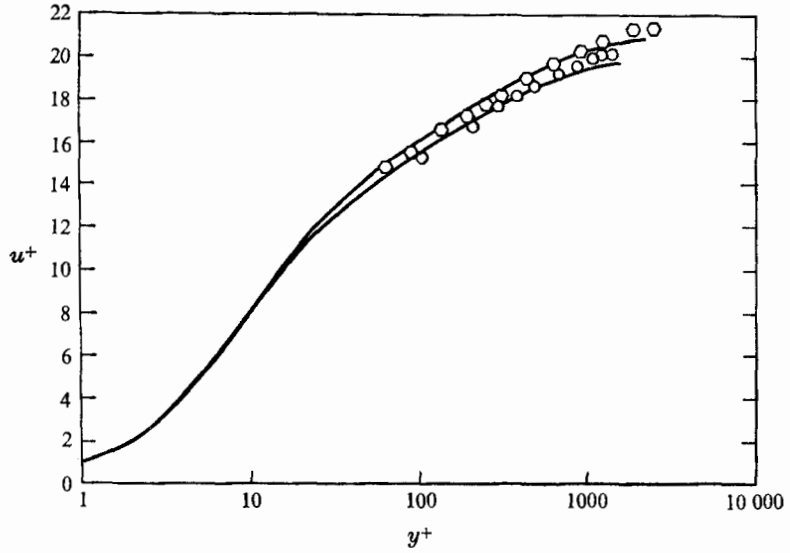

FIGURE 5. Fully developed annular flow (Lawn 1968). ⬡, $\langle \partial\tau^+/\partial y^+ \rangle = -0{\cdot}0015$, $A^+ = 25$, $a^+ = 780$; ○, $\langle \partial\tau^+/\partial y^+ \rangle = -0{\cdot}0023$, $A^+ = 24$, $a^+ = 480$; —, computed velocities.

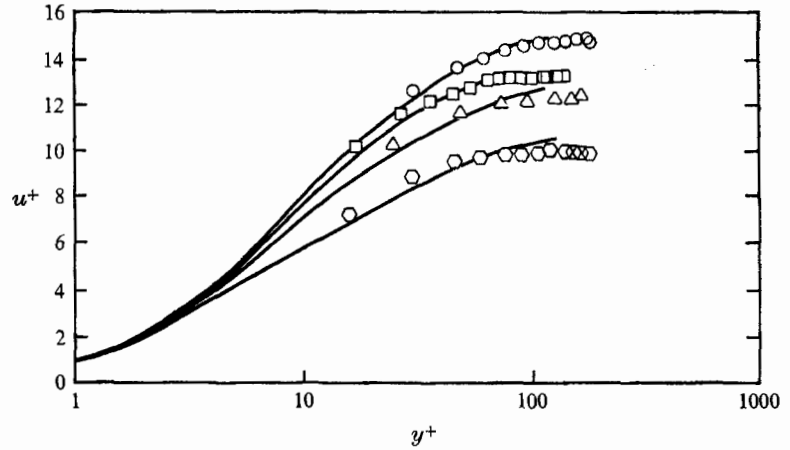

FIGURE 6. Axisymmetric wall jet (Starr & Sparrow 1967). ⬡, $\langle \partial\tau^+/\partial y^+ \rangle = -0{\cdot}0050$, $A^+ = 5{\cdot}70$, $a^+ = 180$; △, $\langle \partial\tau^+/\partial y^+ \rangle = -0{\cdot}0027$, $A^+ = 13{\cdot}0$, $a^+ = 280$; □, $\langle \partial\tau^+/\partial y^+ \rangle = -0{\cdot}0024$, $A^+ = 18{\cdot}0$, $a^+ = 590$; ○, $\langle \partial\tau^+/\partial y^+ \rangle = -0{\cdot}0018$, $A^+ = 21{\cdot}0$, $a^+ = 1000$; —, computed velocities.

The above arguments lead one to expect that A^+ will be a universal function of $\partial\tau^+/\partial y^+$. *If it can be shown that A^+ is virtually constant for the small values of $\partial\tau^+/\partial y^+$ which characterize constant-pressure boundary layers, then the logarithmic law as used by Coles is re-established.* Figure 9 shows the variation of A^+ for a series of two-dimensional flows, i.e. wall jets, channel flows and boundary layers. Since $-\partial\tau^+/\partial y^+$ is about 10^{-3} in the inner layer of a boundary layer for $Re_\theta \approx 1000$ and numerically less at higher Reynolds numbers, it can be concluded that A^+ is virtually constant in boundary layers except perhaps at the very lowest Reynolds numbers, where the flow may not be fully turbulent anyway. This completes our

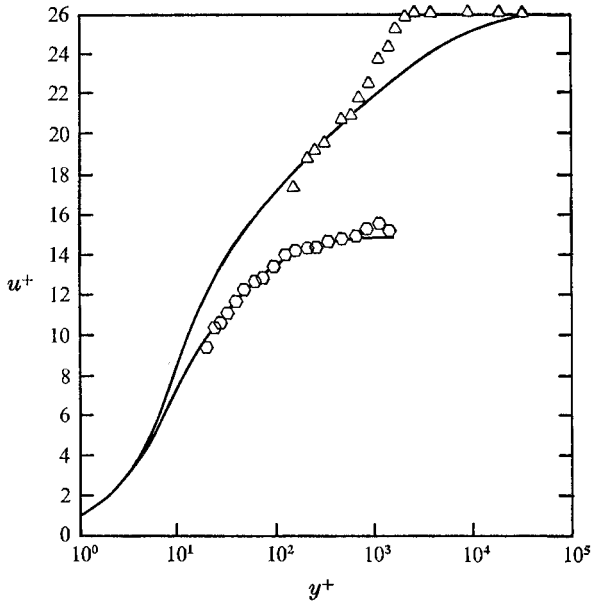

FIGURE 7. Axisymmetric boundary layer (Cebeci 1968). △, $\langle \partial\tau^+/\partial y^+ \rangle = -0{\cdot}00062$, $A^+ = 27$, $a^+ = 1500$; ○, $\langle \partial\tau^+/\partial y^+ \rangle = -0{\cdot}016$, $A^+ = 29$, $a^+ = 17$; —, computed velocities.

demonstration of the validity of the logarithmic law; it is not a perfect demonstration but it does show that the primary effect of external influences on the inner layer is a change in A^+ or C rather than a change in k (see the lowest three curves in figure 4 (*a*), for instance). This seems to dispose of Simpson's suggestion that C varies so as to preserve a close approximation to the original logarithmic profile as k varies; it is much more likely that k and C are constant in boundary layers at low Reynolds numbers.

3. Behaviour of the outer layer

It can be seen from figures 10 and 11 that the velocity defect profiles in duct flows are virtually unaffected by Reynolds number outside the viscous sublayer [noting that (10) implies a constant value of $\tau^+ - \frac{1}{2}y^+$ rather than y^+ for the edge of the sublayer if the two are different]. At the lower Reynolds numbers, the viscous sublayer is so thick that the region of collapse is very small; however, by noting that, in this range of Reynolds number, Re_θ is only about 0·07 of $2\bar{u}a/\nu$, i.e. about $-2/\langle \partial\tau^+/\partial y^+ \rangle$, it is apparent that the outer layer in a pipe or duct is unaffected by viscosity at Reynolds numbers much less than those causing marked changes in the boundary-layer 'wake component' characterized by Π.

Accepting the validity of the logarithmic law implies that the outer-layer Reynolds number effects first noted by Coles (1962) are indeed real. (Simpson's result that $u/u_e = f(y/\delta)$ in the outer layer, coupled with a universal logarithmic law, implies that $\Pi \propto u_e/u_\tau \propto Re_\theta^{-\frac{1}{8}}$, which agrees quite well with Coles' variation for $Re_\theta > 1000$, though not at lower Reynolds numbers.) The most economical hypothesis suggests that the presence of these effects in boundary layers and

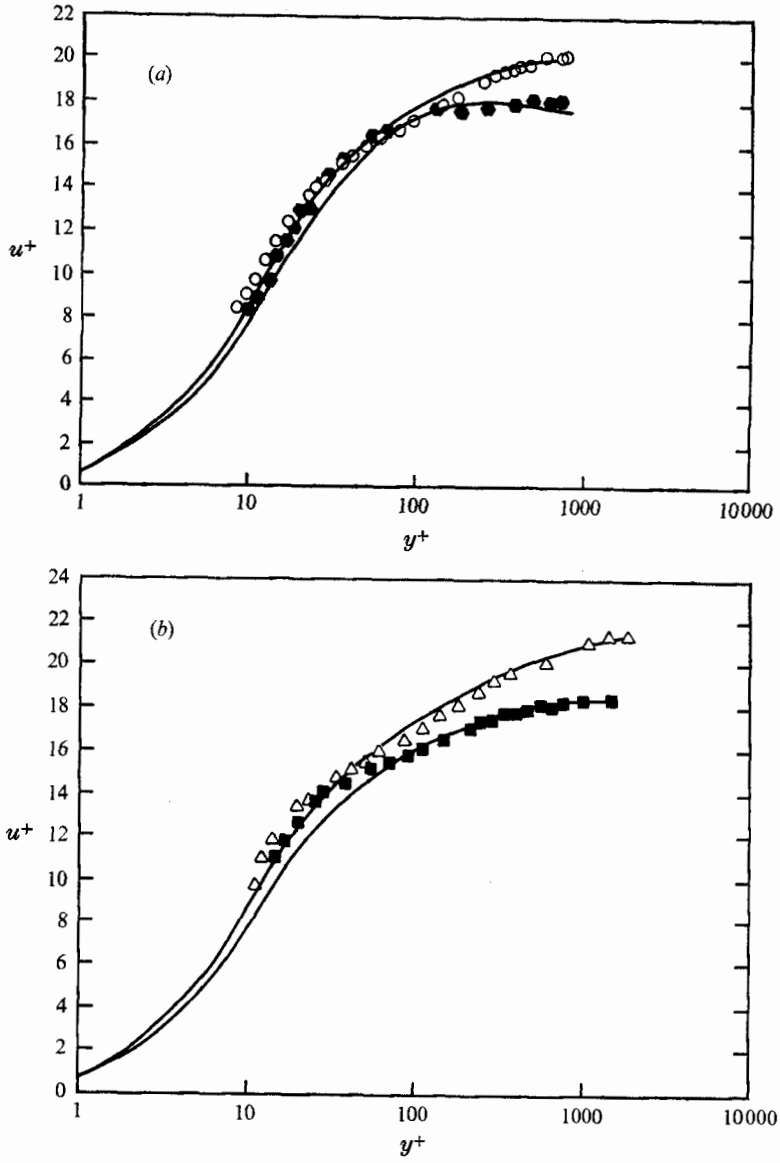

FIGURE 8. Two-dimensional boundary layer (Julien *et al.* 1970). (*a*) ●, $\langle \partial\tau^+/\partial y^+ \rangle = -0{\cdot}018$, $A^+ = 67, \pi^+ = -0{\cdot}0087, v_w^+ = -0{\cdot}0047$; ○, $\langle \partial\tau^+/\partial y^+ \rangle = -0{\cdot}0096, A^+ = 40, \pi^+ = -0{\cdot}012$, $v_w^+ = 0$; —, computed velocities. (*b*) ■, $\langle \partial\tau^+/\partial y^+ \rangle = -0{\cdot}016$, $A^+ = 44$, $\pi^+ = -0{\cdot}0034$, $v_w^+ = -0{\cdot}037$; △, $\langle \partial\tau^+/\partial y^+ \rangle = -0{\cdot}0048$, $A^+ = 35$, $\pi^+ = -0{\cdot}0057$, $v_w^+ = 0$; —, computed velocities.

their absence from pipe and duct flows must be connected with the presence of an interface between the turbulent and irrotational flow in the former case and its absence in the latter case. This interface contains the viscous superlayer, wherein mean and fluctuating vorticity are communicated by viscous action to previously irrotational fluid.

The average thickness of the superlayer, δ_{sup}, is expected to depend, at least to a first approximation, on the mean-square vorticity in the turbulence near the

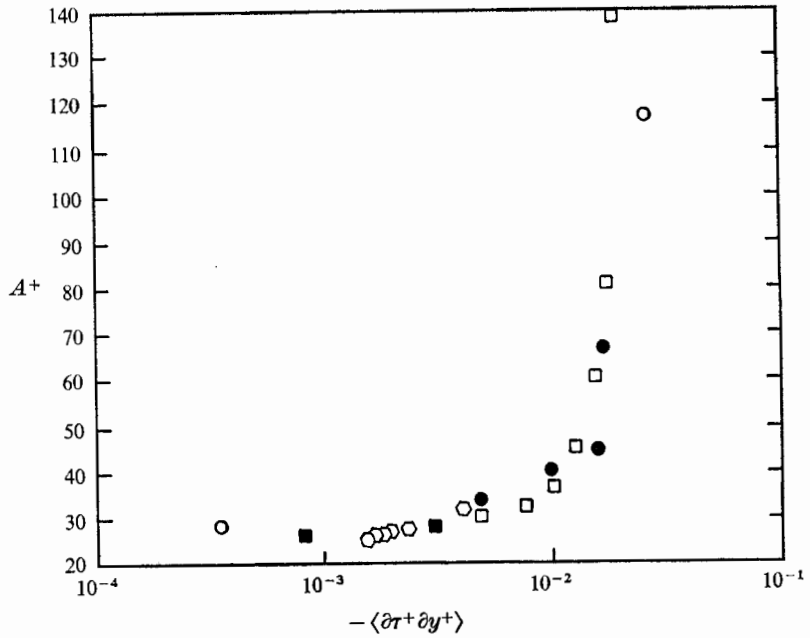

FIGURE 9. The viscous length scale A^+ for two-dimensional flows. Two-dimensional wall jet: ⬡, Bradshaw & Gee (1962). Fully developed channel flow: □, Patel & Head (1969); ■, Laufer (1950). Two-dimensional boundary layers: ○, Badri Narayanan & Ramjee (1969); ●, Julien *et al.* (1970).

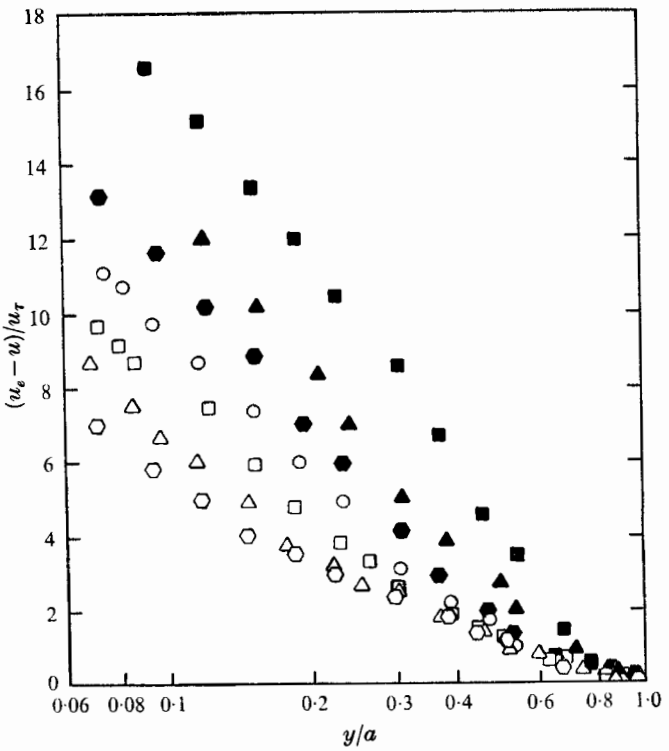

FIGURE 10. Fully developed channel flow (Patel & Head 1969). ⬡, $\langle\partial\tau^+/\partial y^+\rangle = -0{\cdot}0049$; △, $\langle\partial\tau^+/\partial y^+\rangle = -0{\cdot}008$; □, $\langle\partial\tau^+/\partial y^+\rangle = -0{\cdot}010$; ○, $\langle\partial\tau^+/\partial y^+\rangle = -0{\cdot}013$; ⬢, $\langle\partial\tau^+/\partial y^+\rangle = -0{\cdot}015$; ▲, $\langle\partial\tau^+/\partial y^+\rangle = -0{\cdot}017$; ■, $\langle\partial\tau^+/\partial y^+\rangle = -0{\cdot}019$.

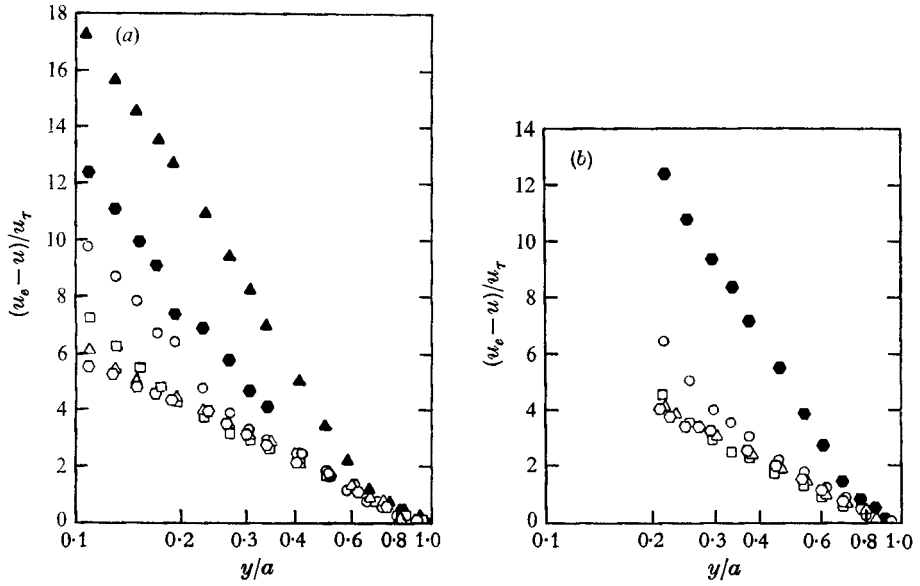

FIGURE 11. Fully developed pipe flow (Patel & Head 1969). (*a*) ○, $\langle \partial\tau^+/\partial y^+ \rangle = -0{\cdot}0034$; △, $\langle \partial\tau^+/\partial y^+ \rangle = -0{\cdot}0042$; □, $\langle \partial\tau^+/\partial y^+ \rangle = -0{\cdot}0065$; ○, $\langle \partial\tau^+/\partial y^+ \rangle = -0{\cdot}0092$; ●, $\langle \partial\tau^+/\partial y^+ \rangle = -0{\cdot}011$; ▲, $\langle \partial\tau^+/\partial y^+ \rangle = -0{\cdot}012$. (*b*) ○, $\langle \partial\tau^+/\partial y^+ \rangle = -0{\cdot}0046$; △, $\langle \partial\tau^+/\partial y^+ \rangle = -0{\cdot}0070$; □, $\langle \partial\tau^+/\partial y^+ \rangle = -0{\cdot}0089$; ○, $\langle \partial\tau^+/\partial y^+ \rangle = -0{\cdot}010$; ●, $\langle \partial\tau^+/\partial y^+ \rangle = -0{\cdot}012$.

superlayer, $\overline{\omega^2}$, and on the viscosity itself. In locally isotropic turbulence, $\overline{\omega^2} = \epsilon/\nu$, where ϵ is the energy dissipation rate, so that δ_{sup} must be approximately proportional to the Kolmogorov length scale $\eta = (\nu^3/\epsilon)^{\frac{1}{4}}$ near the inner boundary of the superlayer. The ratio of the viscous sublayer thickness δ_{sub} to the value of η at $y^+ \approx 40$ is approximately 20; δ_{sup} may also be significantly larger than the local η, which in turn will be significantly larger than η near the sublayer because ϵ is less near the superlayer than near the sublayer. A conservative conclusion is that the superlayer is, at least, not much thinner than the sublayer. The sublayer is plane whereas the superlayer is distributed over a highly irregular interface. Indeed, the irregularity of the interface seems to increase at low Reynolds numbers, judging by the intermittency measurements and smoke photographs of Fiedler & Head (1966). Consequently, the fraction of the boundary-layer fluid that is occupied by the superlayer is much larger than $\delta_{\text{sup}}/\delta$. If $\delta_{\text{sup}}/\delta$ is of the same order as $\delta_{\text{sub}}/\delta$ it is approximately 0·015 at $Re_\theta = 5000$ and 0·1 at $Re_\theta = 600$. Clearly, the superlayer may have a large influence on the outer layer at low Reynolds numbers, and possibly no part of the turbulence in the intermittent region ($y/\delta > 0{\cdot}4$, say) will be independent of viscous effects. This seems the most likely cause of the variation of Coles' II with Re_θ.

4. The effect of transverse curvature

The apparently consistent differences in the values of A^+ for two-dimensional and axisymmetric flow fields with large $|\partial\tau^+/\partial y^+|$ (see figure 12) combined with the apparent constancy of k suggest that transverse curvature may affect the

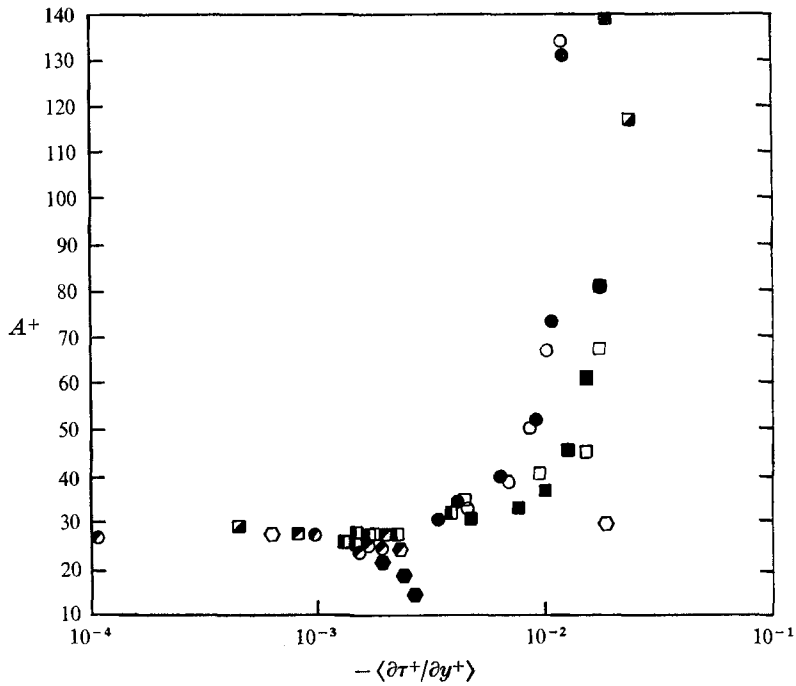

FIGURE 12. The viscous length scale A^+ for two-dimensional and axisymmetric flows. Axisymmetric flows on concave surfaces, fully developed pipe flow: ○, ●, Patel & Head (1969); ◐, Laufer (1954). Two-dimensional flows: ◧, Bradshaw & Gee (1962), two-dimensional wall jet; ■, Patel & Head (1969), fully developed channel flow; ◩, Laufer (1950), fully developed channel flow; □, Julien *et al.* (1970), two-dimensional boundary layers; ◪, Badri Narayanan & Ramjee (1969), two-dimensional boundary layers. Axisymmetric flows on convex surfaces: ⬣, Starr & Sparrow (1967), axisymmetric wall jet; ◐, Lawn (1968), fully developed annular flow; ⬡, Cebeci (1968), axisymmetric boundary layer.

viscous sublayer. However it is generally accepted that transverse curvature does *not* affect the rest of the inner layer (recall that the ratio of the inner-layer thickness to the radius of curvature is independent of Reynolds number and that many high Reynolds number experiments have confirmed that k is the same in circular pipes, plane-wall ducts and boundary layers). The value of $\langle\partial\tau^+/\partial y^+\rangle$ at which the A^+ values start to diverge corresponds to $\delta_{sub}/a \simeq 0{\cdot}1$ whereas the ratio of the inner-layer thickness to a is about 0·2. There being no obvious reason for the observed sensitivity of the viscous sublayer to transverse curvature, some additional data were analysed. These cases consisted of flows on convex surfaces, i.e. flows on the outside of circular cylinders, as well as on concave surfaces. The velocity profiles are plotted in figures 5, 6 and 7 and additional two-dimensional boundary-layer data are shown on figure 8. Figure 12 shows the trends of A^+.

The agreement between the measured and calculated velocity profiles in figures 5–8 is not as good as that of figures 3 and 4; however, it is of sufficient accuracy to ascertain the general trend of the $A^+ - \partial\tau^+/\partial y^+$ relation. The annular duct, axisymmetric wall jet and axisymmetric boundary-layer data clearly show

a trend of A^+ with $\partial\tau^+/\partial y^+$ in the opposite sense to that found in pipes. Note that $\partial\tau^+/\partial y^+$ is dependent on the transverse curvature (see equation (8)) and is thus a suitable curvature parameter itself, at least in flows that change slowly with x.

There are no straightforward explanations of the apparent curvature effect except the most obvious one that it is a real effect of curvature on the sublayer. The consistency of the trend from pipe to duct to annulus seems to rule out arguments based on differences between any two of these flows. A possible clue to the surprising sensitivity of the sublayer to transverse curvature comes from the observation (Kline *et al.* 1967; Gupta *et al.* 1971) of a tendency to transverse periodicity in the sublayer with a wavelength λ given by $u_\tau\lambda/\nu = \tau^+ \approx 100$. Moreover, $\lambda/a \approx 3\delta_{sub}/a \approx 100(\partial\tau^+/\partial y^+)$; consequently, λ/α is about 0.3, i.e. one transverse wavelength subtends about 20°, when significant curvature effects begin. This transverse scale is quite large when compared with the eddy length scales just outside the viscous sublayer, i.e. $l^+_{sub} \approx 16$ when $y^+ \approx 40$, so that it is plausible that the sublayer is affected while the remainder of the inner layer is not.

5. Conclusions

The data analysis of § 2 shows that the logarithmic velocity profile (1) is valid in a wide range of low Reynolds number flows if the dimensionless shear-stress gradient in the inner layer, $\langle\partial\tau^+/\partial y^+\rangle$, is not much greater numerically than 10^{-3}. At larger values of $\langle\partial\tau^+/\partial y^+\rangle$ the best-fit value of the Van Driest damping constant A^+ departs from its basic value of about 26 (figure 9) but the best-fit value of von Kármán's constant k appears to remain at 0·41. Since A^+ represents the effect of the viscous sublayer (it determines the additive constant C in (1)) it is implied that the viscous sublayer is more sensitive to external influences than the fully turbulent part of the inner layer; the generally accepted 'local-equilibrium' analysis for the inner layer (Townsend 1961) suggests that the first effect of external influences will be felt via $\partial\tau/\partial y$, and the consistency of results from different flows for $\langle\partial\tau^+/\partial y^+\rangle$ less than 10^{-3} supports this.

These results contradict Simpson's (1970) suggestion that k and C (or A^+) vary in a constant-pressure boundary layer for $1000 < Re_\theta < 6000$, because $\langle\partial\tau^+/\partial y^+\rangle$ is numerically less than 10^{-3} throughout this range. We based our analysis on flows in which low Reynolds number effects are expected to be larger than in a boundary layer; the data for the boundary layer itself are *not* sufficient to reach a conclusion. Simpson's analysis of Wieghardt's data (Coles & Hirst 1968) contradicts that of Coles (1962) and either analysis produces a worthwhile improvement in calculations of low Reynolds number boundary layers.

The discussion of § 3 suggests that the breakdown of the velocity defect law (2) in the outer layer of a boundary layer at low Reynolds numbers (implied by the analyses of Coles *and* of Simpson) is attributable to the 'viscous superlayer' at the interface separating turbulent and irrotational flow. In pipe and duct flows there is no such interface and the defect law appears to hold at low Reynolds number.

A warning not to credit the complete infallibility of the inner-layer similarity arguments is given by the differences in the best-fit values of A^+ for different

flows at *large* values of $\langle \partial\tau^+/\partial y^+ \rangle$ (figure 12). A^+ appears to depend on the transverse curvature, though there is every reason to believe that k does not. Again it appears that the viscous sublayer is more sensitive to external influences than the fully turbulent part of the inner layer but the reasons for the effect of transverse curvature remain conjectures.

REFERENCES

Badri Narayanan, M. A. & Ramjee, V. 1969 *J. Fluid Mech.* **35**, 225.

Black, T. J. & Sarnecki, A. J. 1958 *Aero. Res. Counc. R. & M.* no. 3387.

Bradshaw, P. & Gee, M. 1962 *Aero. Res. Counc. R. & M.* no. 3252.

Cebeci, T. 1968 *Douglas Aircraft Corp. Paper*, no. 5524.

Cebeci, T. & Mosinskis, G. J. 1970 *Proc. A.S.M.E. Space Technology & Heat Transfer Conference*, part 2.

Cebeci, T. & Smith, A. M. O. 1968 *Douglas Aircraft Division Rep.* DAC 67130.

Coles, D. E. 1962 *Rand Corp. Rep.* R-403-PR.

Coles, D. E. & Hirst, E. A. 1968 *Proc. AFOSR-IFP-Stanford Conference on Turbulent Boundary-Layer Prediction*, vol. 2. Thermosciences Division, Stanford University.

Corrsin, S. & Kistler, A. L. 1955 *N.A.C.A. Rep.* no. 1244.

Fiedler, H. & Head, M. R. 1966 *J. Fluid Mech.* **25**, 719.

Gupta, A. K., Laufer, J. & Kaplan, R. E. 1971 *J. Fluid Mech.* **50**, 193.

Herring, H. J. & Mellor, G. L. 1968 *N.A.S.A. Contractor Rep.* N.A.S.A. CR-1144.

Huffman, G. D. 1971 *Imperial College of Science and Technology Aero Rep.* no. 71-06.

Julien, H. L., Kays, W. M. & Moffat, R. J. 1970 *Stanford University, Department of Mechanical Engineering Rep.* HMT-10.

Kline, S. J., Reynolds, W. C., Schraub, F. A. & Runstadler, P. W. 1967 *J. Fluid Mech.* **30**, 741.

Laufer, J. 1950 *N.A.C.A. Tech. Note*, no. 2123.

Laufer, J. 1954 *N.A.C.A. Rep.* no. 1174.

Lawn, C. H. 1968 *Central Electricity Generating Board Rep.* RN RD/B/N 1232.

McDonald, H. 1969 *J. Fluid Mech.* **35**, 311.

Patankar, S. V. & Spalding, D. B. 1967 *Heat and Mass Transfer in Boundary Layers.* Cleveland: C.R.C. Press. (Also London: Morgan–Grampian.)

Patel, V. C. & Head, M. R. 1969 *J. Fluid Mech.* **38**, 181.

Simpson, R. L. 1970 *J. Fluid Mech.* **42**, 769.

Starr, J. B. & Sparrow, E. M. 1967 *J. Fluid Mech.* **29**, 495.

Townsend, A. A. 1961 *J. Fluid Mech.* **11**, 97.

Van Driest, E. R. 1956 *J. Aero. Sci.* **23**, 1007.

Willmarth, W. W. & Yang, C. W. 1970 *J. Fluid Mech.* **41**, 47.